Chinese Journal of Natural Medicines

Multioxidized polyketides from an endophytic *Penicillium* sp. YUD17006 associated with *Gastrodia elata*

Hongtao LI, Ruining YANG, Fei XIE, Tianpeng XIE, Linhuan TANG, Hao ZHOU, Zhongtao DING

Citation: Hongtao LI, Ruining YANG, Fei XIE, Tianpeng XIE, Linhuan TANG, Hao ZHOU, Zhongtao DING, Multioxidized polyketides from an endophytic *Penicillium* sp. YUD17006 associated with *Gastrodia elata*, Chinese Journal of Natural Medicines, 2024, 22(10), 1−8. doi: 10.1016/S1875−5364(24)60724−7.

View online: https://doi.org/10.1016/S1875−5364(24)60724−7

Available online at www.sciencedirect.com
ScienceDirect
Chinese Journal of Natural Medicines 2024, **22**(11): 1057-1064
doi: 10.1016/S1875-5364(24)60724-7
Chinese Journal of Natural Medicines

•Original article•

Multioxidized polyketides from an endophytic *Penicillium* sp. YUD17006 associated with *Gastrodia elata*

LI Hongtao[2Δ], YANG Ruining[1, 4Δ], XIE Fei[1], XIE Tianpeng[1], TANG Linhuan[1], ZHOU Hao[1*], DING Zhongtao[1, 3*]

[1] *Key Laboratory of Functional Molecules Analysis and Biotransformation of Universities in Yunnan Province, Yunnan Characteristic Plant Extraction Laboratory, School of Chemical Science and Technology, Yunnan University, Kunming 650091, China;*
[2] *School of Pharmaceutical Science & Yunnan Key Laboratory of Pharmacology for Natural Products, Kunming Medical University, Kunming 650500, China;*
[3] *College of Traditional Chinese Medicine, Yunnan University of Chinese Medicine, Kunming 650500, China;*
[4] *Medicinal Plants Research Institute, Yunnan Academy of Agricultural Sciences, Kunming 650200, China*

Available online 20 Nov., 2024

[ABSTRACT] Three novel, highly oxygenated polyketides, multioketides A−C (**1**−**3**), and three previously described multioxidized aromatic polyketides (**4**−**6**), were isolated from an endophytic *Penicillium* sp. YUD17006 associated with *Gastrodia elata*. Their chemical structures were elucidated using extensive spectroscopic data, electronic circular dichroism calculations, and single X-ray diffraction analysis. All metabolites were characterized by a typical *α*,*β*-unsaturated ketone fragment and exhibited a high degree of oxidation. Multioketides A and B were identified as a pair of epimers featuring a rare dihydroisobenzofuranone core. Multioketide C possessed a novel 5/6/6/6 heterotetracyclic chemical architecture with unusual 1,4-dioxin functionalities. Plausible biosynthetic pathways for **1**−**6** were proposed. Additionally, compound **3** demonstrated weak inhibitory activities against both acetylcholinesterase and protein tyrosine phosphatase 1B.

[KEY WORDS] *Penicillium* sp.; Multioxidized polyketides; Secondary metabolite; Anti-acetylcholinesterase activity; PTP1B inhibitory activity

[CLC Number] R284.1 **[Document code]** A **[Article ID]** 2095-6975(2024)11-1057-08

Introduction

A significant proportion of clinically approved small molecular entities originate directly or indirectly from natural products (NPs) [1-3], such as staurosporine (antitumor), fumagillin (antiangiogenic), lovastatin (hypolipidemic), and rapamycin (immunosuppressive) [3, 4]. Among these, fungal polyketides represent a structurally diverse group of naturally occurring small molecules with a wide range of chemical scaffolds and biological activities, which have garnered considerable attention from pharmaceutical chemists and pharmacologists [5-7]. Polyketides incorporating dihydroisobenzofuranone or 1,4-dioxin moieties are relatively rare, especially those originating from fungal NPs [8, 9].

As part of our ongoing research into the microbial chemical diversity associated with the traditional Chinese medicinal herb *Gastrodia elata* Blume (Orchidaceae) [10-13], the fermentation extract of an endophytic *Penicillium* sp. YUD17006 (GenBank OR282480) was phytochemically investigated. This led to the isolation of three highly oxygenated polyketides, multioketides A−C (**1**−**3**), and three previously known multioxidized aromatic polyketides (**4**−**6**) (Fig. 1). Structurally, **1** and **2** represented a new polyketide subtype possessing a relatively rare dihydroisobenzofuran frame-

[Received on] 23-Nov.-2023
[Research funding] This work was supported by the Natural Science Foundation of China (No. 22267001), the Program for Innovative Research Team of Yunnan Province (No. 202105AE160006), the Science and Technology Project of Yunnan Province (Nos. 202201AT070225, 202301AU070217), Yunnan University "Double First-Class" Construction Joint Project (No. 202201BF070001-014), Basic Research Plan of Yunnan Provincial Science and Technology Department-Kunming Medical University (No. 202301AY070001-186), Project of Yunnan Characteristic Plant Screening and R&D Service CXO Platform (No. 2022YKZY001), Key Laboratory of Chemistry in Ethnic Medicinal Resources, State Ethnic Affairs Commission & Ministry of Education, Yunnan Minzu University (No. MZY2205), The Program Innovative Research Team in Science and Technology in Kunming Medical University (No. CXTD202202).
[*Corresponding author] E-mails: haozhou@ynu.edu.cn (ZHOU Hao); ztding@ynu.edu.cn (DING Zhongtao)
[Δ]These authors contributed equally to this work.
These authors have no conflict of interest to declare.

work, while **3** was identified as the first example of a novel 5/6/6/6 heterotetracyclic ring with an unusual 1,4-dioxin core. All compounds were characterized by higher oxidation levels and typical *α*,*β*-unsaturated ketone fragments. Compounds **1**−**3** were tested for their acetylcholinesterase (AChE) inhibitory activity, protein tyrosine phosphatase 1B (PTP1B) inhibitory activity, and cytotoxic activity. The detailed isolation, planar structure identification, stereochemistry determination, putative biosynthetic pathways, and bioassays of metabolites were described.

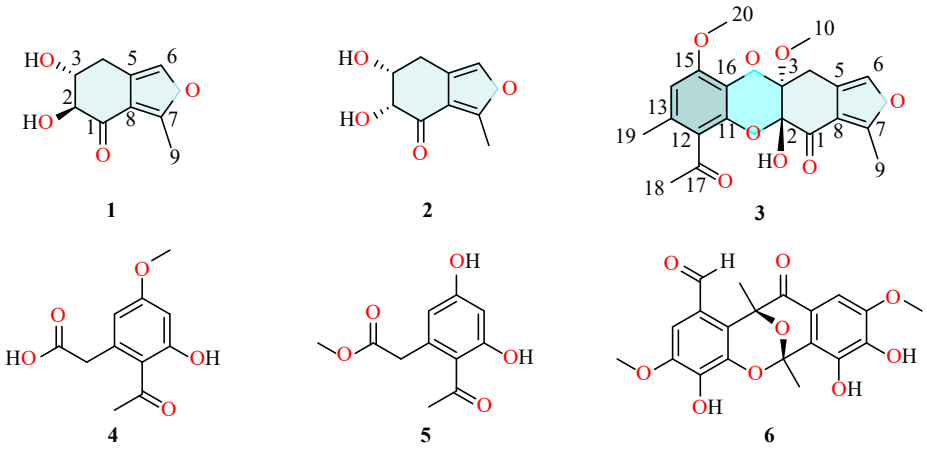

Fig. 1 Chemical structures of compounds 1−6.

Results and Discussion

Structural elucidation

Multioketide A (**1**) was isolated as colorless crystals. Its molecular formula was determined to be $C_9H_{10}O_4$ based on the high-resolution electrospray ionization mass spectrometry (HR-ESI-MS) data $[M + Na]^+$ 205.0463 (Calcd. for 205.0471), corresponding to five indexes of hydrogen deficiency (IHDs). The infrared spectroscopy (IR) spectrum of **1** displayed absorption bands indicative of hydroxyl (3464 cm^{-1}) and carbonyl (1715 cm^{-1}) groups. The ^1H nuclear magnetic resonance (NMR) data (Table 1) revealed characteristic signals for one singlet methyl group at δ_H 2.54 (s), one methylene δ_H [3.11 (dd, J = 15.2, 4.8 Hz), 2.64 (ddd, J = 15.6, 10.4, 2.0 Hz)], two oxygenated methines δ_H [4.02 (d, J = 9.6 Hz), 3.87 (td, J = 10.0, 4.8 Hz)], along with one oxygenated olefin proton signal at δ_H 7.27 (d, J = 2.0 Hz). With the aid of distortionless enhancement by polarization transfer (DEPT) and heteronuclear single quantum coherence (HSQC) spectra, the ^{13}C NMR data (Table 1) of **1** showed nine resonances, assigned as one methyl (δ_C 13.7), one sp^3 methylene (δ_C 28.0), two oxygenated sp^3 methines (δ_C 80.9 and 73.2), one sp^2 methine (δ_C 137.9), and four non-protonated carbons (three sp^2 carbons at δ_C 159.2, 122.1 and 118.0, one ketone carbonyl carbon at δ_C 195.0). The above groups accounted for three out of the five IHDs, indicating that **1** has a bicyclic ring system.

Analysis of the ^1H-^1H correlation spectroscopy (COSY) spectrum (Fig. 2) of **1** revealed a proton spin-coupling system involving H-2/H-3/H_2-4. The C-1 carbonyl carbon was assigned based on the HMBC correlation from H-2 to C-1. Key HMBC correlations of H-6 with C-5, C-7, and C-8, as

Table 1 ^1H NMR (400 MHz) and ^{13}C NMR (100 MHz) spectroscopic data of 1 and 2 in methanol-d_4

No.	1		2	
	δ_H (J in Hz)	δ_C, type	δ_H (J in Hz)	δ_C, type
1	-	195.0, C	-	195.6, C
2	4.02, d (9.6)	80.9, CH	4.40, q (2.8)	78.9, CH
3	3.87, td (10.0, 4.8)	73.2, CH	4.33, d (2.0)	73.5, CH
4	3.11, dd (15.2, 4.8)	28.0, CH_2	2.95, m	27.3, CH_2
	2.64, ddd (15.6, 10.4, 2.0)		-	-
5	-	122.1, C	-	123.2, C
6	7.27, d (2.0)	137.9, CH	7.23, t (1.6)	138.3, CH
7	-	159.2, C	-	158.3, C
8	-	118.0, C	-	118.4, C
9	2.54, s	13.7, CH_3	2.54, s	13.7, CH_3

well as H_3-9 with C-7 and C-8, facilitated the assignment of a 7-methylfuran (ring A) moiety in **1**. Further heteronuclear multiple bond correlations (HMBCs) of H-2 with C-1/C-3 and H_2-4 with C-2/C-3/C-5/C-8 suggested that the dihydroxy cyclohexanone system (ring B) is fused to the methylfuran (ring A) at C-5 and C-8. The relative configuration of **1** was established by the $^3J_{HH}$ coupling constant values. The large $^3J_{2,3}$ and $^3J_{3,4\beta}$ values of 10.0 Hz and the small $^3J_{3,4\alpha}$ value of 4.8 Hz indicated an axial-axial-axial-equatorial relationship for H-2, H-3, H-4β, and H-4α in the cyclohexanone ring [14]. Fortunately, a single crystal of **1** suitable for X-ray diffraction analysis was obtained from MeOH-H_2O (Fig. 3). The structure and stereo-configuration of **1** was established by the X-ray crystallographic diffraction experiment with Cu Kα radiation (CCDC 2051119). Additionally, the electronic circular dichroism (ECD) spectra calculations for (2*S*,3*R*)-**1a**, (2*R*,3*S*)-**1b**, (2*S*,3*S*)-**1c**, and (2*R*,3*R*)-**1d** were performed using the time-dependent density functional theory (TDDFT) method [15]. The experimental ECD spectrum of **1** exhibited positive Cotton effects (CEs) at 280 nm and negative CEs at 230 and 212 nm, which closely matched the calculated spectrum for the (2*S*,3*R*)-**1a** configuration (Fig. 4A1). Accordingly, the structure of **1** was unambiguously determined (Fig. 1).

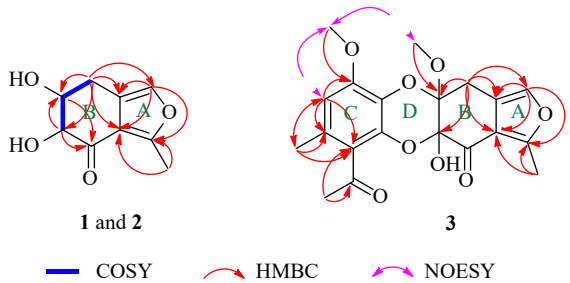

Fig. 2 Key ^{1}H-^{1}H COSY and HMBC correlations of 1–3.

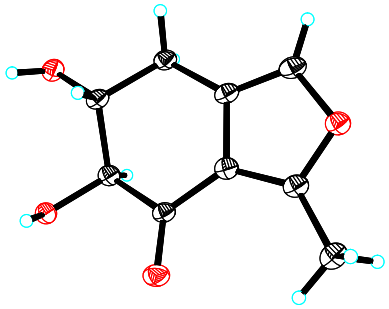

Fig. 3 X-ray ORTEP drawing of multioketide A (1).

The HR-ESI-MS data of compound **2** indicated it has the same molecular formula, $C_9H_{10}O_4$, as compound **1**. Unexpectedly, its ^{13}C NMR spectra closely resembled those of **1** (Fig. 5), with significant chemical shift differences observed near the chiral carbon signal C-2. This observation led us to propose that **2** is an epimer of **1** at C-2. As expected, the relative configurations of C-2 and C-3 were defined as *cis* on the basis of the relatively small coupling constant between H-2 and H-3 ($^3J_{H\text{-}2,H\text{-}3}$ = 2.8 Hz). Moreover, obvious differences in the experimental ECD spectra of **1** and **2** (Fig. 4) suggested the opposite absolute configuration at C-2. Ultimately, the absolute configuration of **2** was assigned as 2*R*,3*R* by matching its calculated and experimental ECD spectra (Fig. 4B1) based on the TDDFT method. Therefore, the structure of compound **2** was defined and named multioketide B (**2**).

Multioketide C (**3**) was acquired as a light yellowish powder with a molecular formula of $C_{20}H_{20}O_8$, as determined by the HR-ESI-MS ion at *m*/*z* 411.1043 $[M + Na]^+$ (Calcd. for $C_{20}H_{20}O_8Na$, 411.1050), corresponding to eleven IHDs. Analysis of the 1D NMR (Table 2) and HSQC spectra (Fig. S18) of **3** revealed the presence of five singlet methyls (two oxygenated δ_C 56.7 and 49.5), one methylene, two sp^2 methines (one oxygenated δ_C 138.4), and twelve non-protonated carbons (two sp^3 carbons at δ_C 99.5 and 93.4, eight sp^2 carbons at δ_C 160.8, 151.3, 141.4, 131.5, 126.9, 124.3, 119.9, and 117.7, along with two ketone carbonyl carbon at δ_C 205.6 and 186.6). Additionally, the structure was inferred to contain tetracyclic ring systems, meeting the molecular formula with eight IHDs.

The skeleton of compound **3** was established by analyzing HMBCs between specific carbons and hydrogens of the previously identified fragments (Fig. 2). Key HMBC correlations of H-6 with C-5, C-7, and C-8, H_3-9 with C-7 and C-8, and H_2-4 with C-2, C-3, C-5, C-6, and C-8 indicated that a furan ring (A) was fused to a cyclohexanone ring (B) *via* a bond between C-5 and C-8, forming a multi-substituted dihydroisobenzofuran moiety (Fig. 2). The existence of a polysubstituted aromatic ring (C) was confirmed by key HMBC cross-peaks from H-14 to C-12, C-13, C-15, and C-19; from H-18 to C-12 and C-17; and from H-19 to C-12, C-13, and C-14 (Fig. 2). The locations of two methoxy groups at C-3 and C-15 were respectively supported by HMBCs from H_3-10 to C-3 and H_3-20 to C-15. The presence of numerous non-protonated carbons and the lack of key HMBCs to connect these two fragments made constructing the complete scaffold of **3** challenging. Considering the atom composition and the eight IHDs, the two moieties must share two oxygen atoms to form a 1,4-dioxin moiety (ring D) [16]. Among the possible ways to assemble ring D, key nuclear Overhauser effect spectroscopy (NOESY) correlations of H_3-10 and H_3-20 indicated that C-3 and C-16 were connected by ether bonds (Fig. 2), implying that C-2 and C-11 were also connected through ether bonds. Combined with the molecular formula, which showed that the only hydroxyl group in the structure was located at C-2, the planar structure of **3** was deduced (Fig. 2).

The relative configuration of compound **3** could not be determined from the NOESY spectrum (Fig. S21). However, considering the spatial hindrance, the relative positions of 10-OCH_3 and 2-OH groups were proposed to be *trans*, resulting in two possible stereoconfigurations of **3**. To further determine the stereochemistry of **3**, all possible isomers, including (2*S*,3*S*)-**3a**, (2*R*,3*R*)-**3b**, (2*S*,3*R*)-**3c**, and (2*R*,3*S*)-**3d**, were calculated using TDDFT-ECD (Fig. 4). The calculated ECD spectrum of (2*S*,3*S*)-**3a** agreed well with the experimental

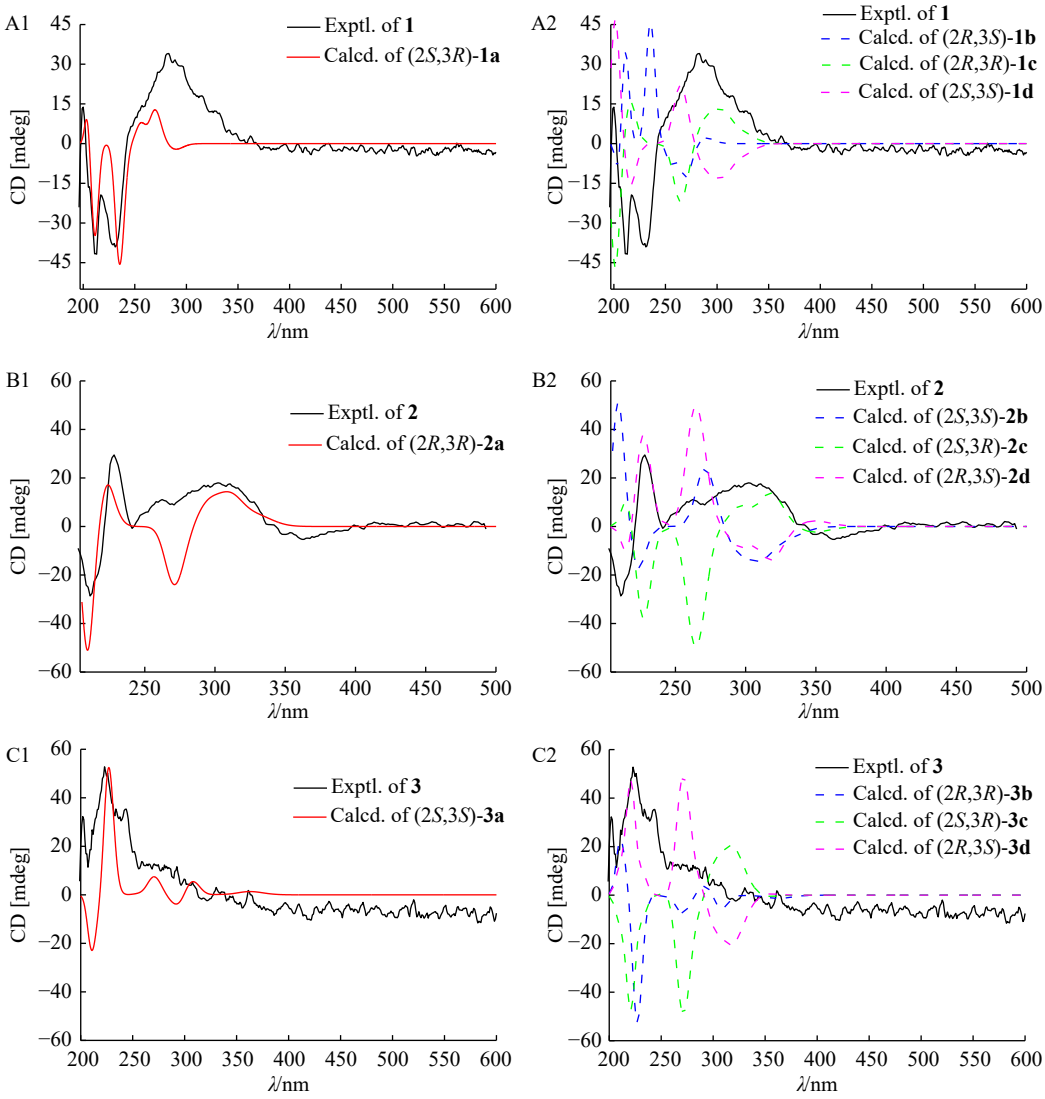

Fig. 4 Experimental and calculated ECD spectra of 1−3 (multioketides A−C).

curve suggesting the absolute configuration of **3** as 2*S*, 3*S*. Thus, **3** was determined as a highly oxygenated aromatic polyketide comprising a novel 5/6/6/6 heterotetracyclic ring system (Fig. 1) and named multioketide C.

Three known multioxidized aromatic polyketides, namely, *O*-menthylcurvulinic acid (**4**) [17], methyl 2-acetyl-3,5-dihydroxyphenylacetate (**5**) [18], and integrastatin B (**6**) [19], were isolated and identified by comparing their observed and reported ESI-MS and NMR data.

Biosynthetic pathway

The plausible biosynthetic pathways for **1**−**6** were postulated in Scheme 1. It is interesting to note that all these isolates showed an obvious chemical relationship among them. Briefly, **2** could be formed through enzymatic epimerization for **1** [20]. Moreover, oxidation of **1** produced key intermediate **i**. **4** could be oxidation and decarboxylation to give key intermediate **ii**. Subsequently, hemiketalization was proposed as a critical step in the formation of **3**, in which the unique 5/6/6/6 heterotetracyclic ring skeleton was constructed by fusing **i** with **ii** through a 1,4-dioxane ring. After selective oxidation and methylation, **4** would be transformed into **5**. The formation of **6** was deduced to involve key Claisen reaction, hemiketalization, selective oxidation, and methylation steps from intermediate **iii** [21].

Biological activity

Fungal polyketides often exhibit significant bioactivities. The new polyketides **1**−**3** were evaluated for their inhibitory activities against AChE *in vitro*. Only **3** exhibited weak activity with an IC_{50} value of 23.7 ± 0.12 μmol·L^{-1} (Table 3), while the positive control tacrine had an IC_{50} of 0.3 ± 0.08 μmol·L^{-1}. Compounds **1**−**3** were also evaluated for their inhibitory activity against PTP1B, a promising therapeutic target for type 2 diabetes mellitus [22]. Compound **3** displayed weak PTP1B inhibitory activity with an IC_{50} value of 32.1 ± 0.23 μmol·L^{-1} (Table 3), where oleanolic acid was used as the positive control (6.8 ± 0.30 μmol·L^{-1}). In addition, we examined the cytotoxic activity of compounds **1**−**3** by the 3-(4,5-dimethylthiazol-2-yl)-2,5-diphenyl tetrazolium bromide

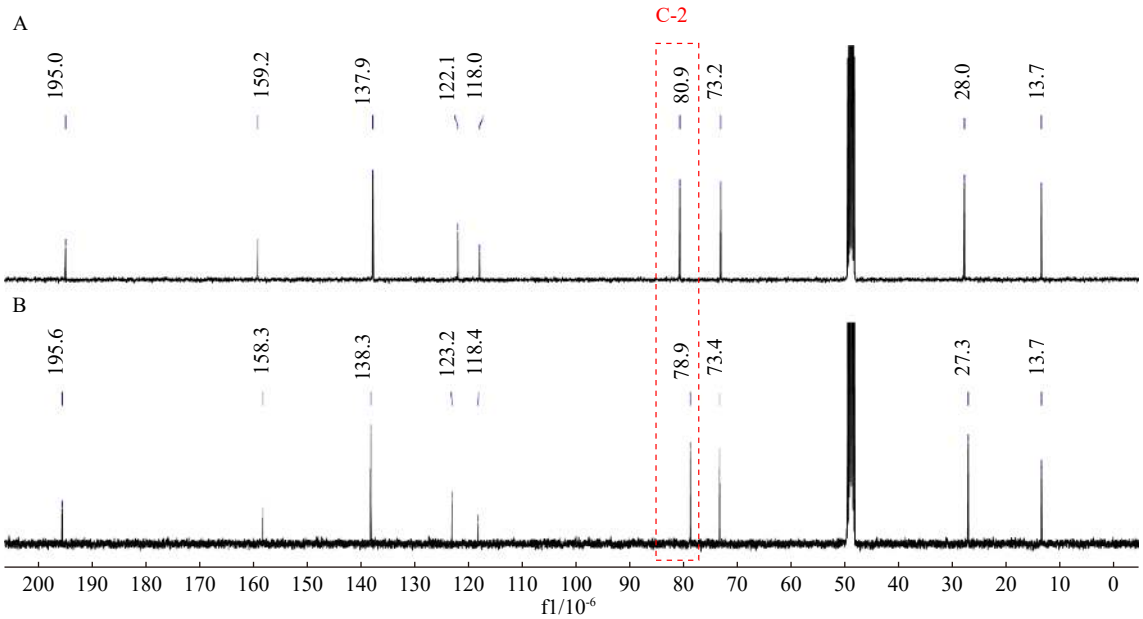

Fig. 5 Comparison of ^{13}C NMR spectra of compounds 1 (A) and 2 (B) from δ_C 0 to 200 × 10^{-6}; 1 and 2 possess very similar carbon chemical shifts; the major deviations between 1 and 2 were the chiral carbon signal C-2.

Table 2 ^{1}H NMR (400 MHz) and ^{13}C NMR (100 MHz) spectroscopic data of 3 in methanol-d_4

No.	δ_H (*J* in Hz)	δ_C, type	No.	δ_H (*J* in Hz)	δ_C, type
1	-	186.6, C	11	-	141.4, C
2	-	93.4, C	12	-	124.3, C
3	-	99.5, C	13	-	126.9, C
4	3.59, d (16.4)	24.3, CH_2	14	6.56, s	108.6, CH
	3.20, d (2.0)			-	-
5	-	119.9, C	15	-	151.3, C
6	7.36, s	138.4, CH	16	-	131.5, C
7	-	160.8, C	17	-	205.6, C
8	-	117.7, C	18	2.65, s	33.1, CH_3
9	2.59, s	13.8, CH_3	19	2.25, s	20.0, CH_3
10	3.16, s	49.5, CH_3	20	3.90, s	56.7, CH_3

(MTT) assay [23]. However, none of the compounds showed significant cytotoxicity against any of the five cancer cell lines tested, including breast cancer MCF-7, colon cancer SW480, hepatocellular carcinoma SMMC-7721, lung cancer A549, and myeloid leukemia HL-60 at a concentration of 40 μmol·L^{-1} (IC_{50} > 40 μmol·L^{-1}).

Conclusions

In summary, three novel multioxidized polyketides, multioketides A−C (**1**−**3**), were discovered from an endophytic *Penicillium* sp. YUD17006 associated with *G. elata*. The anti-AChE activity, PTP1B inhibitory activity, and cytotoxicity of compounds **1**−**3** were screened and discussed. Structurally, multioketides A (**1**) and B (**2**) featured a rare dihydroisobenzofuran-4(5*H*)-one skeleton. Multioketide C (**3**) was characterized by a novel 5/6/6/6 heterotetracyclic ring system featuring the unusual 1,4-dioxin unit. Notably, the structures of

Table 3 Inhibitory effects of compounds 1−3 on PTP1B and AChE (mean ± SD, *n* = 3)

Compounds	IC_{50} (μmol·L^{-1})	
	AChE	PTP1B
1	> 50	> 50
2	> 50	> 50
3	23.7 ± 0.12	32.1 ± 0.23
Tacrine [a]	0.3 ± 0.08	-
Oleanolic acid [a]	-	6.8 ± 0.30

[a] Positive control.

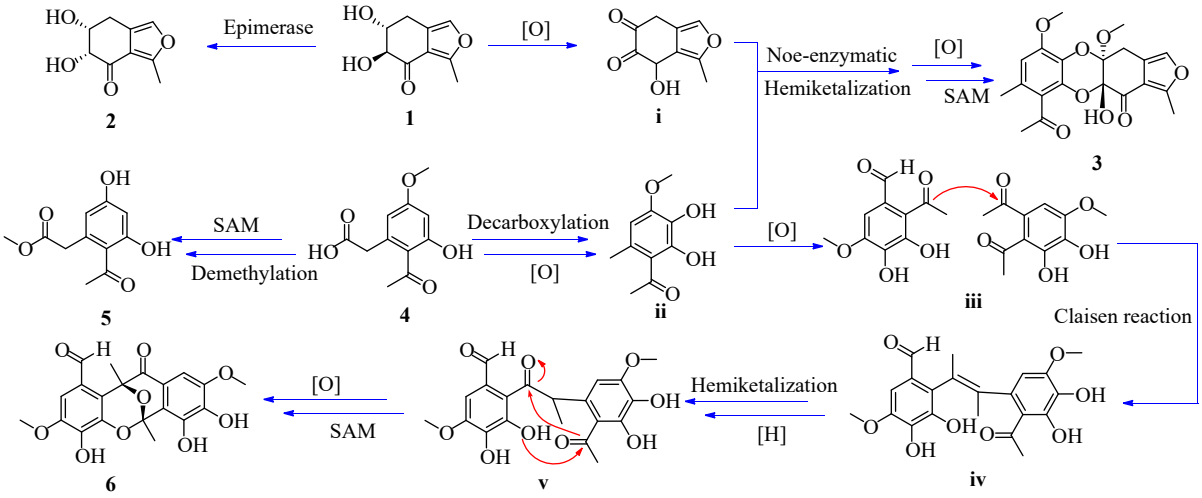

Scheme 1 Plausible biosynthetic pathways of 1−6.

compounds **1**−**6** were characterized by typical *α*,*β*-unsaturated ketone motifs and higher oxidation states, adding a new dimension to the structural diversity of the fungal polyketide family. The biosyntheses of **1**−**6** could proceed similarly as proposed in Scheme 1. These discoveries of metabolites **1**−**6** in the same organism provide new insight into the biosynthesis of aromatic polyketides.

Experimental

General experimental procedures

The melting point was determined on the XRC-1 melting point apparatus. Optical rotations were measured with a JASCO P-1020 digital polarimeter. UV absorption data were obtained in MeOH using a Shimadzu UV-2401PC spectrophotometer. A Nicolet Magna-IR 550 spectrometer was used to record IR spectra (KBr pellets). ECD data were acquired on a JASCO J-810 CD spectrometer. The crystal data of **1** were collected on a Bruker Apex DUO diffractometer with a graphite monochromator using Cu Kα radiation (λ = 1.54178 Å). 1D and 2D NMR spectra were recorded on a Bruker AVANCE (400 MHz for ^{1}H NMR and 100 MHz for ^{13}C NMR) spectrometer, with TMS as the internal standard. An Agilent 1290 UPLC/6545 Q-TOF mass spectrometer was used to collect the HR-ESI-MS data. Column chromatography (CC) was performed on silica gel (200−300 mesh, Qingdao Marine Chemical Inc., Ltd.), Sephadex LH-20 column (GE Healthcare Co.), and Lichroprep reversed-phase (RP)-18 (Merck, 40−60 μm). Thin-layer chromatography (TLC) separations were conducted on precoated glass silica gel GF_{254} plates (Qingdao Marine Chemical Inc., Ltd.).

Fungal material

The fungus strain YUD17006 was isolated from fresh *G. elata* Blume (Orchidaceae), a perennial herb collected in Zhaotong (104°26′1″E, 27°76′9″N), Yunnan Province, China, in November 2020. This fungal strain was identified as *Penicillium* sp. YUD17006 by the sequence analyses of the rDNA internal transcribed spacer (ITS) region using a basic local alignment search tool (BLAST) available on the National Center for Biotechnology Information (NCBI) website [24]. The sequence data have been submitted to GenBank with the accession number OR282480. A reference culture of the strain was maintained at −80 °C in the School of Chemical Science and Technology, Yunnan University, China.

Scale-up fermentation and isolation

The strain *Penicillium* sp. YUD17006 was cultured on a potato dextrose agar (PDA) plate at 25 °C for 7 days. The mycelia and spores were scraped into 500 mL Erlenmeyer flasks with 150 mL of potato dextrose broth (PDB) medium and incubated on a rotary shaker (180 r·min^{-1}) at 28 °C for 3 d. For scale-up fermentation, the seed culture was transferred into 100 × 500 mL Erlenmeyer flasks with 200 mL of PDB medium and incubated on a rotary shaker (180 r·min^{-1}) at 28 °C for 14 d. The fermentation broth (20 L) and mycelia were extracted with ethyl acetate (EtOAc) and acetone, respectively. The extractions were combined and evaporated under reduced pressure to yield a gum (7.8 g).

The extract was subjected to a silica gel CC using successive elution of $CHCl_3$−MeOH mixtures (100 ∶ 0, 50 ∶ 1, 30 ∶ 1, 10 ∶ 1, and 1 ∶ 1, *V*/*V*) to yield five fractions (Fr. A−Fr. E) as determined by TLC analysis. Fr. B was separated using Sephadex LH-20 CC (MeOH) to give four subfractions (Fr. B.1−Fr. B.4). The subfraction Fr. B.2 was subjected to silica gel CC eluting with a stepwise gradient of PE−EtOAc (50 ∶ 1 to 1 ∶ 1, *V*/*V*) to afford compound **3** (5.0 mg). The subfraction Fr. B.2 that eluted with CH_2Cl_2−MeOH (55 ∶ 1, *V*/*V*) was subjected to a Sephadex LH-20 column, eluting with MeOH to yield compounds **1** (8.0 mg) and **2** (4.5 mg). Fr. C was separated by Sephadex LH-20 (MeOH) to yield five fractions (Fr. C.1−Fr. C.5). Fr. C.1 was subjected to reversed-phase (RP)-C_{18} CC using MeOH−H_2O (3 ∶ 7 to 10 ∶ 1, *V*/*V*) and further purified using Sephadex LH-20 CC with MeOH to generate compound **6** (12.5 mg). Compound **5** (9.0 mg) was obtained from fraction Fr. C.3, which was purified by over RP-C_{18} silica gel CC eluted with MeOH−H_2O (1 ∶ 1, *V*/*V*). Fr. C.5 was further refined by CC eluting with a

CH_2Cl_2–MeOH gradient (from 30 ∶ 1 to 5 ∶ 1, *V/V*) and silica gel CC with PE–EtOAc (3 ∶ 1, *V/V*) to obtain compound **4** (6.0 mg).

Compound Characterization

Multioketide A (1)

Colourless crystal; mp: 96–97 °C; HR-ESI-MS *m/z* 205.0463 $[M + Na]^+$ (Calcd. for $C_9H_{10}O_4Na$, 205.0471); $[\alpha]_D^{21}$ +5.84 (*c* 0.11, MeOH); IR (KBr) ν_{max}: 3464, 1715, 1642, 1375, and 1105 cm^{-1}; UV (MeOH) λ_{max} (log ε): 204 (0.91), 224 (0.49), and 278 (0.28) nm; ^1H and ^{13}C NMR data (methanol-d_4) (Table 1).

Multioketide B (2)

Colourless solid; HR-ESI-MS *m/z* 205.0469 $[M + Na]^+$ (Calcd. for $C_9H_{10}O_4Na$, 205.0471); $[\alpha]_D^{21}$ −0.51 (*c* 0.20, MeOH); IR (KBr) ν_{max}: 3452, 1716, 1630, 1375, and 1108 cm^{-1}; UV (MeOH) λ_{max} (log ε): 204 (0.82) and 276 (0.19) nm; ^1H and ^{13}C NMR data (methanol-d_4) (Table 1).

Multioketide C (3)

Light yellowish powder; HR-ESI-MS *m/z* 411.1043 $[M + Na]^+$ (Calcd. for $C_{20}H_{20}O_8Na$, 411.1050); $[\alpha]_D^{21}$ +9.49 (*c* 0.13, MeOH); IR (KBr) ν_{max}: 3425, 2847, 1674, 1603, 1460, 1337, 1268, 1148, and 883 cm^{-1}; UV (MeOH) λ_{max} (log ε): 200 (1.02), 224 (0.72), and 274 (0.47) nm; ^1H and ^{13}C NMR data (methanol-d_4) (Table 2).

Crystallographic data of multioketide A (1)

Suitable crystals of **1** were obtained from a mixed solvent of MeOH–H_2O (50 ∶ 1, *V/V*). $C_9H_{10}O_4$, Mr = 182.17, a = 6.2042(3) Å, b = 16.7706(7) Å, c = 30.6539(14) Å, α = 90°, β = 90°, γ = 90°, V = 3189.5(3) $Å^3$, T = 100.(2) K, space group *P*212121, Z = 16, μ(Cu Kα) = 1.019 mm^{-1}, 53808 reflections measured, 6295 independent reflections (R_{int} = 0.1034), final R_1 = 0.0748 ($I > 2\sigma(I)$), final $wR(F^2)$ = 0.2032 ($I > 2\sigma(I)$), final R_1 = 0.0821 (all data), final $wR(F^2)$ = 0.2130 (all data), goodness of fit on F^2 = 1.077, and flack parameter = 0.17(9) (CCDC 2051119).

ECD computations

All quantum-chemical calculations were performed using the Gaussian 09 program package. Conformational searches of compounds **1**–**3** were performed in CONFLEX 8.0 software based on molecular mechanics with the Merck molecular force field (MMFF). The conformations with lower energetics were further optimized at the B3LYP/6-311 + G (d, p) level in the Gaussian 09 package [25]. The calculated ECD spectra of compounds **1**–**3** were generated through TDDFT calculations at the B3LYP/6-311 + G (2d, p) level using the polarizable continuum model (PCM) in methanol solution [15]. The overall ECD curve of each conformer was weighted by the Boltzmann distribution after UV correction using SpecDis 1.71 software.

AChE inhibitory assay

AChE inhibitory activity was assessed based on the spectrophotometric method developed by Ellman *et al.* with slight modifications [26]. Briefly, the enzymatic reaction was conducted in a reaction system consisting of 0.35 U·mL^{-1} AChE (Sigma-Aldrich), 20 μL of 1.05 mmol·L^{-1} acetylthiocholine iodide (ATCh) and 40 μL of 0.02 mol·L^{-1} (pH 8.0) phosphate-buffered saline (PBS) in 96-well microplates, which were incubated for 30 min at 37 °C. DMSO solutions of the tested compounds were added to the assay solution and incubated for 5 min, followed by the measurement of absorbance at 405 nm using a plate reader. Tacrine was used as a positive control. All reactions were performed in triplicate.

PTP1B inhibition assay

PTP1B inhibitory activity was determined by measuring the activity of the enzyme through the rate of hydrolysis of *p*-nitrophenyl phosphate (*p*NPP) [22]. Briefly, compounds **1**–**3** (10 μmol·L^{-1}) and the positive control oleanolic acid (10 μmol·L^{-1}) were pre-incubated with the enzyme at 25 °C for 5 min. In a typical 100 μL assay mixture containing 50 mmol·L^{-1} 3-morpholinopropanesulfonic acid (MOPs), 2 mmol·L^{-1} *p*NPP, and 30 nmol·L^{-1} PTP1B, activities were continuously monitored. The reaction was terminated by adding 2 mol NaOH (10 μL) after incubation at 37 °C for 30 min. The amount of produced pNP was monitored at an absorbance of 405 nm wavelength, and IC_{50} values were calculated.

Cytotoxicity assay

The MTT assay [23] was performed to evaluate cytotoxicity against MCF-7, SW480, SMMC-7721, A549, and HL-60 cell lines. The IC_{50} values were assessed based on the dose-response curve by Reed and Muench's method, with cisplatin used as a positive control.

Supporting Materials

NMR and MS spectra for all compounds are available as Supporting Information and can be requested by sending an E-mail to the corresponding author.

References

[1] Wright GD. Opportunities for natural products in 21st century antibiotic discovery [J]. *Nat Prod Rep*, 2017, **34**(7): 694-701.
[2] Crawford J, Korman T, Labonte J, *et al*. Structural basis for biosynthetic programming of fungal aromatic polyketide cyclization [J]. *Nature*, 2009, **461**(7267): 1139-1143.
[3] Truax NJ, Romo D. Bridging the gap between natural product synthesis and drug discovery [J]. *Nat Prod Rep*, 2020, **37**(11): 1436-1453.
[4] Newman DJ, Cragg GM. Natural products as sources of new drugs over the nearly four decades from 01/1981 to 09/2019 [J]. *J Nat Prod*, 2020, **83**(3): 770-803.
[5] Zang Y, Gong Y, Shi Z, *et al*. Multioxidized aromatic polyketides produced by a soil-derived fungus *Penicillium canescens* [J]. *Phytochemistry*, 2022, **193**: 113012.
[6] Lin Z, Phadke S, Lu Z, *et al*. Onydecalins, fungal polyketides with anti-histoplasma and anti-TRP activity [J]. *J Nat Prod*, 2018, **81**(12): 2605-2611.
[7] Li X, Chen HP, Zhou L, *et al*. Cordycicadins A–D, antifeedant polyketides from the entomopathogenic fungus *Cordyceps cicadae* JXCH1 [J]. *Org Lett*, 2022, **24**(47): 8627-8632.
[8] Lin J, Liu S, Sun B, *et al*. Polyketides from the ascomycete fungus *Leptosphaeria* sp. [J]. *J Nat Prod*, 2010, **73**(5): 905-910.
[9] Ding WY, Yan YM, Meng XH, *et al*. Isolation, total synthesis, and absolute configuration determination of renoprotective di-

meric *N*-acetyldopamine-adenine hybrids from the insect *Aspongopus chinensis* [J]. *Org Lett*, 2020, **22**(15): 5726-5730.
[10] Li HT, Yang RN, Liu T, *et al*. Fungal polyketides from a rhizospheric soil-derived *Penicillium* sp. YUD17004 associated with *Gastrodia elata* [J]. *Phytochemistry*, 2023, **205**: 113475.
[11] Li HT, Tang L, Liu T, *et al*. Polyoxygenated meroterpenoids and a bioactive illudalane derivative from a co-culture of *Armillaria* sp. and *Epicoccum* sp. [J]. *Org Chem Front*, 2019, **6**(23): 3847-3853.
[12] Li HT, Zhou H, Duan RT, *et al*. Inducing secondary metabolite production by co-culture of the endophytic fungus *Phoma* sp. and the symbiotic fungus *Armillaria* sp. [J]. *J Nat Prod*, 2019, **82**(4): 1009-1013.
[13] Li HT, Sun Y, Xie F, *et al*. Xanthene and citrinin derivatives from the endophytic fungus *Penicillium* sp. T2-11 [J]. *Tetrahedron Lett*, 2022, **90**: 153626.
[14] Trana TD, Wilson BAP, Henrich CJ, *et al*. Structure elucidation and absolute configuration of metabolites from the soil-derived fungus *Dictyosporium digitatum* using spectroscopic and computational methods [J]. *Phytochemistry*, 2020, **173**: 112278.
[15] Pescitelli G, Bruhn T. Good computational practice in the assignment of absolute configurations by TDDFT calculations of ECD spectra [J]. *Chirality*, 2016, **28**(6): 466-474.
[16] Zang Y, Gong YH, Li XW, *et al*. Canescones A−E: aromatic polyketide dimers with PTP1B inhibitory activity from *Penicillium canescens* [J]. *Org Chem Front*, 2019, **6**(18): 3274-3281.
[17] Ying YM, Zhang LW, Shan WG, *et al*. Secondary metabolites of *Peyronellaea* sp. XW-12, an endophytic fungus of *Huperzia serrata* [J]. *Chem Nat Compd*, 2014, **50**: 723-725.
[18] Varma GB, Fatope MO, Marwah RG, *et al*. Production of phenylacetic acid derivatives and 4-epiradicinol in culture by *Curvularia lunata* [J]. *Phytochemistry*, 2006, **67**: 1925-1930.
[19] Singh SB, Zink DL, Quamina DS, *et al*. Integrastatins: structure and HIV-1 integrase inhibitory activities of two novel racemic tetracyclic aromatic heterocycles produced by two fungal species [J]. *Tetrahedron Lett*, 2002, **43**: 2351-2354.
[20] Tshitenge DT, Feineis D, Awale S, *et al*. Gardenifolins A-H, scalemic neolignans from *Gardenia ternifolia*: chiral resolution, configurational assignment, and cytotoxic activities against the HeLa cancer cell line [J]. *J Nat Prod*, 2017, **80**(5): 1604-1614.
[21] Zang Y, Gong Y, Gong J, *et al*. Fungal polyketides with three distinctive ring skeletons from the fungus *Penicillium canescens* uncovered by OSMAC and molecular networking strategies [J]. *J Org Chem*, 2020, **85**(7): 4973-4980.
[22] Xie FZ, Yang FZ, Liang YY, *et al*. Investigation of stereoisomeric bisarylethenesulfonic acid esters for discovering potent and selective PTP1B inhibitors [J]. *Eur J Med Chem*, 2019, **164**: 408-422.
[23] Gerlach SL, Dunlop RA, Metcalf JS, *et al*. Cyclotides chemosensitize glioblastoma cells to temozolomide [J]. *J Nat Prod*, 2022, **85**(1): 34-46.
[24] Shao M, Sun C, Liu X, *et al*. Upregulation of a marine fungal biosynthetic gene cluster by an endobacterial symbiont [J]. *Commun Biol*, 2020, **3**(1): 527.
[25] Sun L, Li W, Li J, *et al*. Uncommon diterpenoids from the south China sea soft coral *Sinularia humilis* and their stereochemistry [J]. *J Org Chem*, 2021, **86**(4): 3367-3376.
[26] Ellman GL, Courtney KD, Andres V, *et al*. A new and rapid colorimetric determination of acetylcholinesterase activity [J]. *Biochem Pharmacol*, 1961, **7**(2): 88-95.

Cite this article as: LI Hongtao, YANG Ruining, XIE Fei, *et al*. Multioxidized polyketides from an endophytic *Penicillium* sp. YUD17006 associated with *Gastrodia elata* [J]. *Chin J Nat Med*, 2024, **22**(11): 1057-1064.